

SPACE CHARGE STUDIES FOR THE IONISATION PROFILE MONITORS FOR THE ESS COLD LINAC

C.A. Thomas*, European Spallation Source ERIC, Lund, Sweden
 F. Belloni, J. Marroncle, CEA, Saclay, France

Abstract

In this paper, we present the results from a numerical code developed to study the effect of space charge on the performance of Ionisation Profile Monitors. The code has been developed from the analytical expression of the electromagnetic field generated by a 3D bunch of charged particles moving along one axis. This transient field is evaluated to calculate the momentum gained by a test moving particle, but not necessary co-moving with the bunch, and included in a non-linear ordinary differential equation solver (Runge-Kutta) to track the 3D motion of the test particle. The model of the IPM is complete when an additional constant electric field is included to project the test particle onto a screen. The results from this code, modelling the IPM to be developed for the ESS Cold Linac, are presented here, and the impact of the space charge on the measurement of the beam profile is discussed.

INTRODUCTION

One of the challenges brought by high power beam such as provided by the ESS linac is that they can damage or simply destroy any material they interact with. For the measurement of transverse beam profile in two orthogonal axis, established method such as Wire-Scanners can not be applied as the wire breaks under a too long interaction with the beam. At ESS to palliate this, Non-invasive Profile Monitors (NPMs) will be in use for all beam with a pulse longer than 50µs and with a 62.5 mA peak current. NPM as called for ESS are based on the interaction between the residual gas chamber and the proton beam, which gives rise to ionisation and to fluorescence of the gas particles. In the superconducting cavities section of the Linac, NPMs use the ionisation byproduct of the interaction. An NPM at ESS is then composed of two orthogonal instruments called Ionisation Profile Monitors, IPM. This instrument is composed of a High-Voltage cage, which project on choice the ions or electrons produced by the proton beam, onto a screen where the beam profile is detected and read-out. One of the issues with this instrument is that its performance depends on the linearity of the projection. The projectiles being charged particles, they will be also interacting with the electromagnetic field generated by the proton bunches. Therefore, high charged bunches are likely to give an addition transverse to the projectiles, giving an error to the read position of the projected projectile. In this paper, we present a numerical code based on a model of the IPM. With this code we investigate the effect of the space charge on the profiles, showing the range of application of the IPM to the ESS beam.

* cyrille.thomas@esss.se

MODEL OF THE IPM AND NUMERICAL MATLAB IMPLEMENTATION

The simple numerical model to investigate the influence of the bunched proton beam of ESS on the IPM performance is described by Eq. 1

$$m \frac{d\vec{v}}{dt} = \vec{F} \quad (1)$$

and with m the mass of the particle, \vec{v} its speed in 3D, and \vec{F} the 3D force felt by the particle.

In the case of the force to be generated by a bunch of charged particles moving at the relative speed in one direction that we choose to be given by the unit vector \mathbf{z} , one can write the force \vec{F} as:

$$\vec{F} = q \left(\vec{E} + \vec{v} \times \vec{B} \right) = q \begin{cases} \left(1 - \beta_b \frac{v_z}{c}\right) E_x \\ \left(1 - \beta_b \frac{v_z}{c}\right) E_y \\ E_z + \beta_b \left(E_x \frac{v_x}{c} + E_y \frac{v_y}{c}\right) \end{cases} \quad (2)$$

where q is the charge of the particle, and $\vec{v} = v_x \hat{\mathbf{x}} + v_y \hat{\mathbf{y}} + v_z \hat{\mathbf{z}}$, the speed of the particle in 3D; $\beta_b = v_b/c$ the relativistic speed of the bunch, and c the speed of light; $\hat{\mathbf{i}}$ represents the unit vector in the lab frame.

The field generated by the relativistic bunch moving along z axis is given by [1]:

$$\vec{E} = \begin{pmatrix} E_x \\ E_y \\ E_z \end{pmatrix} = \begin{pmatrix} \gamma_b \bar{E}_x \\ \gamma_b \bar{E}_y \\ \bar{E}_z \end{pmatrix} \quad (3)$$

with $\gamma_b = \frac{1}{\sqrt{1-\beta_b^2}}$ the Lorentz factor related to the bunch relativistic speed. $\vec{E} = \bar{E}_x \mathbf{x} + \bar{E}_y \mathbf{y} + \bar{E}_z \mathbf{z}$ is the field generated by the bunch in the rest frame coordinate of the bunch, with its origin in the center of the bunch and with unit vectors $\hat{\mathbf{i}}$ collinear to $\hat{\mathbf{i}}$, and in which the coordinates transform as:

$$\bar{x} = x \quad \bar{y} = y \quad \bar{z} = \gamma_b (z - \beta_b ct) \quad (4)$$

and the dimensions of the 3D Gaussian bunch we consider here is:

$$\bar{\sigma}_x = \sigma_x \quad \bar{\sigma}_y = \sigma_y \quad \bar{\sigma}_z = \gamma_b \sigma_z \quad (5)$$

The expression of the 3D field generated by the 3D Gaussian bunch is given by:

$$\vec{E} = \frac{Q_b}{4\pi\epsilon_0} \frac{1}{\sqrt{\pi}} \begin{pmatrix} \int_0^\infty dq \frac{2\bar{x}}{q_x^{3/2}} \frac{1}{\sqrt{q_y q_z}} e^{-\frac{\bar{x}^2}{2q_x} - \frac{\bar{y}^2}{2q_y} - \frac{\bar{z}^2}{2q_z}} \\ \int_0^\infty dq \frac{2\bar{y}}{q_y^{3/2}} \frac{1}{\sqrt{q_x q_z}} e^{-\frac{\bar{x}^2}{2q_x} - \frac{\bar{y}^2}{2q_y} - \frac{\bar{z}^2}{2q_z}} \\ \int_0^\infty dq \frac{2\bar{z}}{q_z^{3/2}} \frac{1}{\sqrt{q_x q_y}} e^{-\frac{\bar{x}^2}{2q_x} - \frac{\bar{y}^2}{2q_y} - \frac{\bar{z}^2}{2q_z}} \end{pmatrix} \quad (6)$$

with

$$q_x = q + \sigma_x^2, q_y = q + \sigma_y^2, q_z = q + \sigma_z^2$$

The function evaluated the field as given by Eq. 6 is implemented in Matlab and is used to solve the motion equation of particles of charge q and mass m , distributed initially with the transverse bunch distribution and linearly along the axis motion, moving under the force F given by the field of the 3D Gaussian bunch and an external field applied in the y direction. This code is implemented in Matlab, and uses the non-linear Runge-Kutta solver for the Ordinary Differential Equation (ODE) described by 1.

Benchmarking

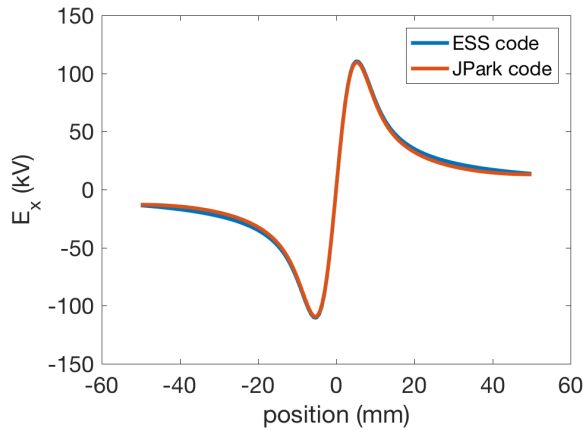


Figure 1: Benchmark of the bunch electric field.

The numerical code is validated by means of benchmarking against analytic solutions and other numerical code, and finally experimental measurements. The first check was performed on the expression of the bunch electric field. The field for a Gaussian bunch has been generated by CST¹, within a collaboration working on modeling IPMs [2]. A comparison with the Gaussian bunch generated by CST and the expression 3 for the case of the PS at CERN is shown in the Figure 1. All aspects of the field have been check, including numerical artifacts. The bunch characteristics for the benchmark against other codes are chosen to be the PS bunch at 26 GHz: r.m.s transverse size, $\sigma_{x,y} = 3.4 \text{ mm} \times 1.4 \text{ mm}$, bunch length, $\sigma_z = 750 \text{ ps}$ ($\sigma_z \approx 224.8 \text{ mm}$); number of protons, 1.33×10^{11} . The model for the calculation of the field is based in both numerical code on a 3D Gaussian distribution, however, the one difference is in our case the bunch

¹ Courtesy of K. Satou - J-Parc, CST: <https://www.cst.com>.

extends to infinity, and in the benchmarking code, the field extension is calculated by means of the Dirichlet bounding condition, which is at $x = \pm 50 \text{ mm}$ in this case. This can probably explain the difference that can be observed on the figure, and which is of the order of 10%. The agreement in the centre of the bunch, and where the intensity is maximum is better than 3%. Therefore, our model applies well to beam propagating in large beam pipe diameter, which is the case for the ESS Linac.

Once the implementation of the Eq. 6 is validated, we also check for the correct implementation of Eq. 1. In our model, the bunch moves at given speed, and periodically repeats, disappearing and re-appearing at each end of the bunch trajectory along the axis \hat{z} at the distance $D = T_0/2 \times \beta_b c$. The position of the bunch is located depending on the time, which is set by the ODE solver.

RESULTS FOR THE ESS BEAM

Table 1: Characteristics of the ESS Proton Beam in the Cold Linac Sections

Beam property	Min.	Max.
Transverse r.m.s size (mm)	0.5	10
Longitudinal Bunch r.m.s size (mm)	0.5	1.3
Energy (MeV)	90	2000
Protons per Bunch	10^8	10^9
RF frequency (MHz)	352.54	
Pulse length (ms)	2.86	

In order to investigate the impact of the space charge on the performance of the IPM under design for the ESS Cold Linac sections, simulation using the code describe above have been done using the ESS beam parameters, and for two kind of particles, electrons and H^+ . The beam parameters used for the simulations are shown in the Tab. 1. The external field of the IPM cage is set to be constant everywhere and only an Electric field is applied. In the design of some other IPM, an additional magnetic field co-linear to the electric field is applied [3,4]. This is not the case for the ESS design, mainly due by the lack of space available at the location of the IPMs. The intensity of the electric field is varied between 50 kV/m and 1000 kV/m. The longitudinal bunch length does not vary significantly for the nominal lattice, and assuming all the cavities perfectly tuned. However, we also varied the bunch length between 0.5 mm and 10 mm, in order to probe the impact of the bunch length on the transverse profile IPM measurement.

Proton Beam Space Charge on Electrons

Figures 2 and 3 present part of our first results selected to illustrates some of the main features of the interaction between the cold plasma and the proton beam. We have selected here initial condition with a round beam of r.m.s

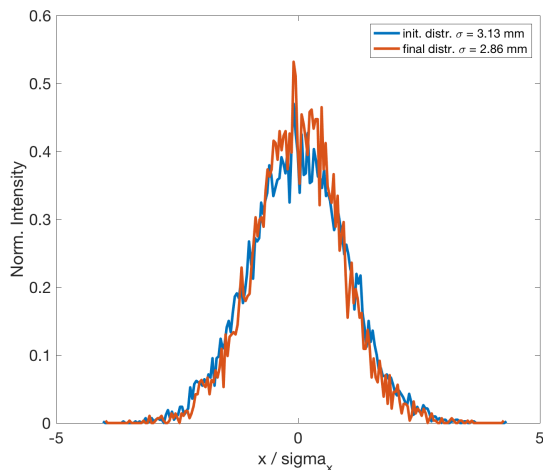


Figure 2: Distribution of electrons on the screen and at initially Gaussian distributed with a r.m.s $\sigma_{x,y} = 3.2$ mm

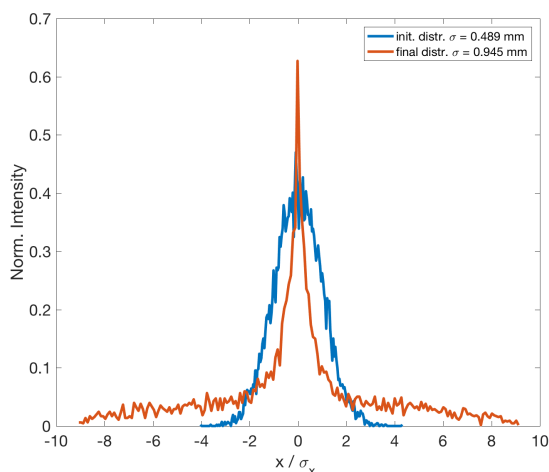


Figure 3: Distribution of electrons on the screen and at initially Gaussian distributed with a r.m.s $\sigma_{x,y} = 0.5$ mm

Gaussian size $\sigma_{x,y} = 0.5$ mm, and $\sigma_{x,y} = 3.2$ mm respectively. The rest of the initial parameters are given in the Tab. 1. The initial Gaussian distributions for each of these simulation is also shown for comparison with the profile measured in the IPM. We also normalised the distribution so that its integral is equal to 1. The space charge effect on opposite charged particles from the charge of the beam, and projected by the IPM HV cage is somehow a focusing effect. The particles are attracted towards the center of the beam while been projected towards the screen. For large r.m.s beam values, typically larger than $\sigma_{x,y} = 3$ mm, and for the large enough field strength, here it is 300 kV/m, the projection seems to be converging to a point rather far from the screen, see Fig. 4. The trajectories do not cross each others, so the final distribution at the screen is smaller, but by only a few percent, as seen in the Fig. 2.

For smaller beam sizes than 3 mm and very small beam as illustrated in Fig. 3, the space charge effect is strong. The

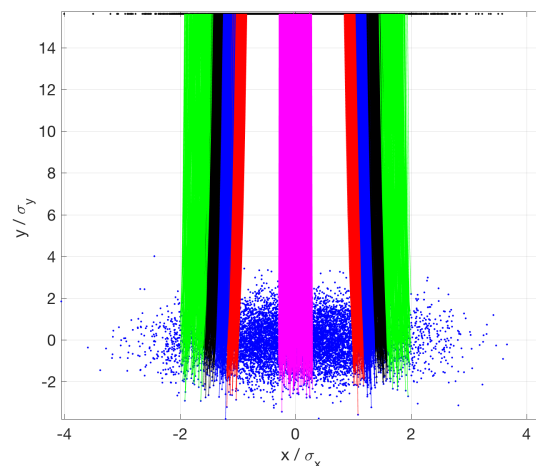


Figure 4: Distribution of electrons on the screen and at initially Gaussian distributed with a r.m.s $\sigma_{x,y} = 3.2$ mm. The colors of the trajectories represent particles for which their initial position is within a slice of the beam, in the center, $|x| < 0.2\sigma_x$ (magenta), in the strongest field positions, $\sigma < |x| < 1.2\sigma$ (red), $1.2\sigma < |x| < 1.4\sigma$ (blue), $1.4\sigma < |x| < 1.6\sigma$ (black), $1.6\sigma < |x| < 2\sigma$ (green).

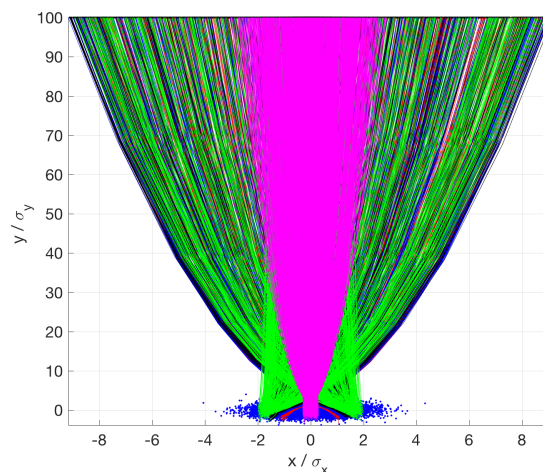


Figure 5: Distribution of electrons on the screen and at initially Gaussian distributed with a r.m.s $\sigma_{x,y} = 0.5$ mm. The sliced colored trajectories are the same as in Fig. 4.

distribution at screen is no longer Gaussian. The trajectories as shown in Fig 5, with the same color code for the slices as in Fig. 5, converge and the initial positions have been projected symmetrical to the centre of the beam. So the distribution at screen although not Gaussian remains symmetric. The final r.m.s size is twice as the initial one.

Proton Beam Space Charge on H^+

Similar space charge effects can be observed on the ions. we focus here on the H^+ species, produced from the ionisation of H_2 molecules, main species in the vacuum chambers residual gas. We have been performing the same simulations

as for the electrons, with the same or within the same range initial beam sizes conditions. The trajectories are repulsed, as expected from the same charged particle as the charge of the beam combined with the HV cage electric field. The resulting r.m.s size distribution is shown in the Fig. 6. The sizes are normalised to the initial beam size, and plotted as function of the initial beam sizes, and for several HV field strength². The values remain under 10% of the initial values for high field strength and for beam larger than 2-3 mm. For smaller beam size, the high field strengths selected for the simulation are not strong enough and the space charge effect is driving the motion of the ions.

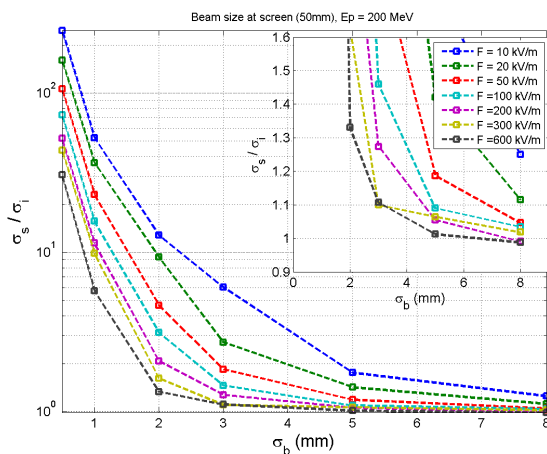


Figure 6: Size of the H⁺ distribution for which the mean value along the E-field axis equals the screen one. The screen position is at 50 mm from the centre of the beam axis. The protons energy is 200 MeV. The profile are retrieved from the projections of the particles projection on the virtual screen, at a time when the centre of mass of the particles is at the screen

DISCUSSION AND CONCLUDING REMARKS

For both particles type, electrons and protons, the proton beam with the ESS characteristics seems to have the same

² The ending conditions between the electron and proton simulation are different: with electrons, the distribution is calculated for particles positions at the screen provided by the implementation of the 'events' function for the Matlab ODE solver; for the proton simulations, we had an earlier 'events' function implemented, and the distribution comes from the projection of the particles positions at the time the proton cloud center of mass as reached the screen

effects: for beam sizes larger than 3 mm, the effect is to distort slightly the distribution. The effect leads to a calculated r.m.s size within 10% of the initial beam size conditions. For smaller beam sizes, the effect is stronger, and the distortion is more pronounced until it is not Gaussian anymore. The question remains whether the distorted distribution can be used to retrieve the initial beam size. An initiative to do so has been started [5]. It is now continued within this development of IPMs for the ESS beam. The trajectories may be characteristic enough to enable the retrieval of the initial beam sizes. There are several approaches we intend to investigate. One is to generate a large look-up table, comparing the resulting distributions. A similar approach has been done for the evaluation of the beam size measured by means of coded apertures [6]. Another approach would be to use a specific transformation, which would lead to a deconvolution method. Both approach will be studied, with the objective to enable the retrieval of the beam size as measured by the IPM is the range of the r.m.s beam sizes from 0.5/mm up to 10 mm and beyond.

REFERENCES

- [1] R Wanzenberg. Nonlinear Motion of a Point Charge in the 3D Space Charge Field of a Gaussian Bunch. Technical Report May, DESY, 2010.
- [2] Mariusz Sapinski et al. Ionization profile monitor simulations - status and future plans. In *IBIC*, 2016, this conference: TUPG71.
- [3] R. Connolly, P. Cameron, W. Ryan, T.J. Shea, R. Sikora, and N. Tsoupas. A prototype ionization profile monitor for rhic. In *PAC*, pages 2152–2154, 1997.
- [4] K. Satou, N. Hayashi, S. Lee, and T. Toyama. a Prototype of Residual Gas Ionization Profile Monitor for J-Parc RCS. In *EPAC*, pages 1163–1165, 2006.
- [5] Jan Egberts. *IFMIF-LIPAc Beam Diagnostics: Profiling and Loss Monitoring Systems put*. PhD thesis, Paris Sud, 2012.
- [6] J.P. Alexander, A. Chatterjee, C. Conolly, E. Edwards, M.P. Ehrlichman, E. Fontes, B.K. Heltsley, W. Hopkins, A. Lyncaker, D.P. Peterson, N.T. Rider, D.L. Rubin, J. Savino, R. Seeley, J. Shanks, and J.W. Flanagan. Vertical beam size measurement in the cesr-ta storage ring using x-rays from synchrotron radiation. *Nuclear Instruments and Methods in Physics Research Section A: Accelerators, Spectrometers, Detectors and Associated Equipment*, 748:96 – 125, 2014.